ISSN 0915-633X

NATIONAL INSTITUTE FOR FUSION SCIENCE

The Effect of Magnetic Field Configuration on Particle Pinch Velocity in Compact Helical System (CHS)

H. Iguchi, K. Ida, H. Yamada, K. Itoh, S.-I. Itoh, K. Matsuoka, S. Okamura, H. Sanuki, I. Yamada, H. Takenaga, K. Uchino and K. Muraoka

(Received – Dec. 15, 1993)

NIFS-267 Jan. 1994

RESEARCH REPORT
NIFS Series

NAGOYA, JAPAN

The Effect of Magnetic Field Configuration on Particle Pinch Velocity in Compact Helical System (CHS)

H. Iguchi, K. Ida, H. Yamada, K. Itoh, S.-I. Itoh#, K. Matsuoka, S. Okamura,
H. Sanuki, I. Yamada
National Institute for Fusion Science, Nagoya 464-01, Japan
#Research Institute for Applied Mechanics, Kyushu University, Kasuga 816, Japan
and
H. Takenaga, K. Uchino, K. Muraoka
Department of Energy Conversion, Kyushu University, Kasuga 816, Japan

Abstract

Radial particle transport has been experimentally studied in the low-aspect-ratio heliotron/torsatron device CHS. A non-diffusive outward particle flow (inverse pinch) is observed in the magnetic configuration with the magnetic axis shifted outward, while an inward pinch, like in tokamaks, is observed with the magnetic axis shifted inward. This change in the direction of anomalous particle flow is not due to the reversal of temperature gradient nor the radial electric field. The observation suggests that the particle pinch velocity is sensitive to the magnetic field structure.

Keywords
anomalous particle transport, particle pinch velocity, non-diffusive particle flow, CHS heliotron/torsatron, magnetic configuration

Studies on anomalous transport in magnetically confined plasmas have been the main issue of fusion research for more than two decades. Developments of experimental techniques and analysis have provided more detailed knowledge on local transport properties in various operational regimes in tokamaks and in stellarators (Wagner et al 1993). An approach using a transport matrix, in which the particle, momentum and heat flows are related with radial gradients of corresponding physical quantities in the matrix form, has been widely discussed for modelling transport phenomena. If the transport is dominated by diffusive processes, the matrix could be expressed only by diagonal elements. However, the observation on the density profile has shown a particle pinch term in particle transport processes. The magnitude of the pinch is larger than the prediction of the neoclassical theory (Ware 1970). The temperature gradient is theoretically expected to drive the anomalous particle pinch flux (Coppi et al 1978).

The recent finding of the various improved confinement mode has clarified the favorable influence of the peaked density profile on the global energy confinement (Greenwald et al 1984, Strachan et al 1987, Gehre et al 1988, Söldner et al 1988). This suggests the importance of understanding the pinch phenomena (Itoh 1990). More recently a heat pinch for electrons is observed in ECH experiments in DIII-D (Luce et al 1992). A momentum pinch for ions is also observed in JFT-2M (Ida et al 1993) and JT-60U (Nagashima et al 1993). It is important to study the relation between these pinch processes and the other gradient forces, which can be a touchstone of various transport modelling.

In this letter, we report the observation of a non-diffusive outward particle flow (inverse pinch) in the neutral beam heated plasma in Compact Helical System (CHS). The pinch phenomena can be studied without being influenced by the neoclassical Ware pinch in the plasma confined without applying the loop voltage. It is found that the particle pinch velocity changes its sign depending on the position of the vacuum magnetic axis. This fact implys that the particle pinch is related with the magnetic field structure, because the shift of magnetic axis change the ripple and shear of the magnetic field. This change of sign is not associated with the change of temperature gradient nor the radial electric field.

CHS is a low-aspect-ratio heliotron/torsatron device with $l = 2$, $m = 8$ helical windings (Nishimura et al 1990), with a major radius of 1 m and an average plasma radius of 0.2 m. The experiments have been carried out at the magnetic field strength at 0.9 T and 1.4 T. Quasi-steady-state plasmas with the average electron density around 2×10^{13} cm^{-3} are sustained by tangential neutral beam injection with port through power of 0.5 - 0.7 MW. In order to study the effect of magnetic configuration on the particle transport, the position of the vacuum magnetic axis is changed in the range from R_{ax} = 89.9 cm to 101.6 cm. This shift of the plasma, relative to helical windings, changes the helical ripple on axis, $\varepsilon_h(0)$, from 2 % to 8 %; $\varepsilon_h(0)$ vanishes at R_{ax} = 94.9 cm. The magnetic hill covers entire region of the plasma radius for inward shift of the magnetic axis. On the other hand, in the position of the magnetic axis at R_{ax} = 96 cm or outer, a magnetic well is formed in the core region. However the helical ripple of l -1 component increases, which should enhance neoclassical transport.

The energy of the neutral beam is high (36 keV) enough to give the considerable shift of the drift orbits for fast ions from the magnetic surfaces in CHS. This shift strongly influences the power deposition profiles. The shift of the drift orbit with respect to the magnetic surface is outward for co-injection of neutral beam (anti-parallel to the magnetic field direction), while it is inward for counter-injection.

Radial profiles of various plasma parameters are measured in the steady state phase of discharges. The electron density and temperature profiles are measured by a single point, scannable Thomson scattering system. The ion temperature profiles and toroidal and poloidal rotation profiles are measured by charge exchange spectroscopy (CXS) using the heating beam. Radial electric field profile is obtained from the toroidal and poloidal rotation velocities using the momentum balance equation.

In order to find the radial particle flux, toroidal and poloidal variations of local neutral hydrogen densities are measured (Uchino et al 1992). Three diagnostic techniques are used. A tunable dye laser to induce H_α emission is used to measure the local hydrogen atom density inside the plasma. Optical fibre arrays (an 8 channel toroidal array and two sets of 34 channel poloidal arrays) are used to measure H_α or H_β emission profiles toroidally and poloidally. Care is taken not only for the poloidal asymmetry but also for the toroidal nonuniformity. A calibrated TV camera with an H_α interference filter measures the toroidal variation of the H_α emission profile. Particle source profiles of recycling and gas puffing are determined with the help of the DEGAS neutral particle simulation code (Heifetz 1986). Birth profiles and slowing down processes of the fast ions from the injected neutral beam are calculated using the transport code PROCTR-MOD (Howe 1990). Finally the radial particle fluxes averaged over magnetic surfaces are derived.

Figure 1 shows the characteristics of the plasma profiles as a function of the position of the vacuum magnetic axis operated with counter-injection of the neutral beam at 0.9 T. Here the peaking parameter for the electron density and temperature profiles is defined as the central value divided by the volume averaged one. The electron density profile is found to be peaked with the inward shifted magnetic axis, while it is flattened with the outward shifted one. From the global confinement point of view, the optimum position of the vacuum magnetic axis is R_{ax} = 92.1 cm (Kaneko et al 1991). Although the real magnetic axis is shifted outward by an amount of 2-3 cm due to Shafranov shift (Yamada et al 1992), it does not influences the discussion. We refer the position of the magentic axis by the vacuum one in the figure. The temperature profile becomes slightly peaked by the inward shift of the magnetic axis, but not as much as the electron density profile. The toroidal rotation velocity is centrally peaked and strongly depends on the position of the magnetic axis, which is explained by the neoclassical parallel viscosity due to helical ripples (Ida et al 1991a). On the other hand, the poloidal rotation velocity, which mainly contribute to radial electric field E_r, increases at the plasma edge. It has been found that E_r is always negative (directed inward) for NBI heated plasmas (Ida et al 1991b). The electron and ion thermal diffusivities are evaluated at the half of plasma minor radius. They only have weak dependence on the position of the magnetic axis. It is clear from those data that the influence of magnetic configuration on the transport processes predominatly appears in the particle transport.

Similar dependences of the density peaking parameter and the toroidal/poloidal rotation velocities on the position of the vacuum magnetic axis have been observed for co-injection as shown in Fig. 1 (a) and (c). The observed peaking parameter of $n_e(0)/<n_e> = 2$ is in the range of those for co-injection in tokamaks (Gehre at al 1988, Ida et al 1992). The strong density peaking, which occurs for counter-injection in tokamaks, has not yet been observed in CHS.

Understanding the particle transport needs quantitative evaluation of the radial particle flux. The neutral particle distributions are measured for two typical magnetic configurations with R_{ax} = 92.1 cm and 99.5 cm at 1.4 T. The plasma is sustained by co-injected neutral beam (R_{ax} = 92.1 cm) or by counter-injected neutral beam (R_{ax} =

99.5 cm). The stored energies for the two cases are comparable. Recycled hydrogen atoms can penetrate into the core plasma and the resultant particle source in the centeral plasma is comparable to the particle source from the injected beam. Figure 2 shows the comparison of the electron temperature and density profiles and radial particle fluxes averaged over magnetic surfaces for the two cases. It is shown that the difference of the electron density profile is remarkable, while the electron temperature profiles are similar. It is noted that the particle source penetrates well into the core region for both cases and the radial particle fluxes are comparable.

The radial particle flux Γ is expressed as

$$\Gamma = -D\nabla n - V_{in} n$$

where D is the particle diffusivity and V_{in} is the inward pinch velocity. In the case of peaked density profile at Rax=92.1 cm, the pinch term and the diffusive term are evaluated from the two time sliced data of density gradient and particle flux. Assuming that the transport coefficients are constant in time between the two phases, the pinch velocity and the particle diffusivity are obtained (Takenaga et al 1993). They are estimated to be $V_{in} = 2$ m/s (inward pinch) and the particle diffusivity is $D = 0.4$ m^2/s at $r/a = 0.7$. Overall error for those values are estimated to be factor 2.

The flattened density profile cannot be explained by the diffusive term only if the hollow profile is sustained in steady state. The figure 2 shows that the particle flow is outward while the density gradient is positive in the region of $0.4 < r/a < 0.8$. This observation demonstrates that there is a non-diffusive outward particle flux. The flow velocity is calculated at $r/a = 0.7$ to be - 4 m/s, using the data of $\Gamma = 6 \times 10^{19}$ $m^{-2}s^{-1}$ and $n_e = 2.4 \times 10^{19}$ cm^{-3} and assuming $D = 0.4$ m^2/s. It is noted that the slightly hollow density profile cannot be attributed to transient phenomenon. The time scale of the change of the local electron density at radius r can be evaluated as

$$\tau(r) = \frac{\int n(r)dr^3}{\Gamma S}$$

where S is the area of plasma surface at radius r. It is calculated to be 20 ms at r/a = 0.7 for Rax = 99.5 cm. The Thomson scattering measurement is done 30 ms after the constant gas puff to make sure that the measurement is in steady state phase. It is concluded that the particle pinch velocity changes its sign depending on the magnetic configuration.

The dependence on the magnetic field strength is studied at Rax = 92.1 cm. The pinch velocity and the diffusivity increase to be 4 m/s and 1 m^2/s as the magnetic field strength decreases for fixed heating power.

For the parameters at r/a = 0.7 of Fig. 2, the collisionality is in the plateau regime. The neoclasical prediction of particle flux is much smaller than the experimental observation. Therefore, this observed particle flux is dominated by the anomalous transport. In the theoretical model of the anomalous transport using a transport matrix, flows can be related with gradient forces as follows;

$$\begin{pmatrix} \Gamma \\ P_{jr} \\ q \end{pmatrix} = -\overleftrightarrow{M} \cdot \begin{pmatrix} \nabla n/n \\ \nabla V_j/v_{the} \\ \nabla T/T \end{pmatrix}$$

where Γ, P_{jr} and q are radial particle, momentum and heat flows, respectively, and M is the transport matrix. Here the pinch process is expressed in terms of off-diagonal elements. Finding practical expressions for the matrix elements is necessary to understand anomalous transport (for example, Balescu 1991, Itoh 1992).

According to the pinch theory (Hazeltine et al 1981, Itoh 1990), the particle flow is expressed as

$$\Gamma = - Dn \left[\frac{\nabla n}{n} + \alpha \frac{\nabla T}{T} - \left(\frac{eE_r}{T} - \left\langle \frac{r\omega}{m} \right\rangle \frac{eB}{cT} \right) \right]$$

where D is positive definite. The numerical factor α is of the order of unity and $\langle r\omega/m \rangle$ is the average phase velocity of the turbulence. It is important to examine the relation between the observed pinch velocity and the gradient forces due to T_e' and E_r. In this model the pinch term can change its sign when (1) $\alpha T'$ changes sign or (2) $[eE_r/T - \langle r\omega/m \rangle eB/cT]$ changes sign. Table 1 shows the comparison of related physical quantities for the two cases. The sign of T' and E_r is unchanged in this experiment. Simplified treatment of anomalous transport (such as Coppi at al 1978) seems not sufficient. Fluctuations with their characters dependent on the magnetic configuration are the possible canadidate to explain the results, which are remained for future study.

It is worth while to compare the dependence of pinch velocity on the magnetic field strength to that for tokamaks. It is shown above that both pinch velocity and diffusivity in CHS are roughly proportional to B^{-1}. In tokamaks, however, those quantities are scaled as I_p^{-1} rather than B^{-1} (Wagner et al 1993). The similar difference between roles of B and I_p was found in the energy transport (Yamada et al 1991), suggesting an intrinsic difference of the anomalous transport in these two configurations.

Finally we discuss on the effect of this convective flow on the global confinement. From the plasma stability point of view, the magnetic configuration with the outward shifted magnetic axis is preferable due to magnetic well formation in the core region. The energy loss rate due to the energy flow of $(5/2)nTV_{in}$ for $R_{ax} = 99.5$ cm is estimated to be 50 s^{-1}. Since the total energy loss rate is calculated to be 330 s^{-1} from the global confinement time of 3 ms in this density regime, this convective loss process contribute to 15 % of the total energy loss. While the convective energy flow is inward for R_{ax} = 92.1 cm, which is calculated to be 7.5 % of the total energy loss. The result indicates that this convective process is not negligibly small in total power balance.

In this letter, it is discussed that particle pinch process can change its sign depending on the magnetic configuration. It is not explained by the change of temperature gradient nor radial ellectric field. The present results may suggest the possibility that the heat pinch process may have a similar dependence on the magnetic configuration, stimulating future research in this field.

The authors wish to thank to those staffs who have contributied to CHS operation, ECH and RF plasma production and neutral beam injection. We also thank to Professor Ohbiki of Plasma Physics Laboratory, Kyoto University for giving us a chance to use a tunable dye laser of Heliotron-E group.

References

Balescu R 1991 Phys. Fluids **B3** 564

Coppi B et al 1978 Phys. Rev. Lett. **21** 551

Greenwald M et al 1984 Phys. Rev. Lett. **53** 352

Gehre O et al 1988 Phys. Rev. Lett. **60** 1502

Hazeltine R D et al 1981 Phys. Fluids **24** 1164

Heifetz D B 1986 Physics of Plasma-Wall Interactions in Controlled Fusion eds. D. E. Post and Behrisch (Plenum, New York) p 675

Howe H C 1990 Research Report of Oak Ridge National Laboratory ORNL/TM-11521

Ida K et al 1991a Phys. Rev. Lett. **67** 58

------------ 1991b Phys. fluids **B3** 515 and **B4** 1360

------------ 1992 Phys. Rev. Lett. **68** 182

------------ 1993 Research Report of Nationa Institute for Fusion Science NIFS-241

Itoh S-I 1990 J. Phys. Soc. Jpn. **59** 3431

----------1992 Phys. Fluids **B4** 796

Kaneko O et al 1988 Plasma Physics and Controlled Nuclear Fusion Research, Proc. 13th Int. Conf. 1990 (Washington) vol 2 (Viena: IAEA) p474

Luce T C et al 1992 Phys. Rev. Lett. **67** 52

Nagashima K et al 1993 submitted to Nucl. Fusion

Nishimura K et al 1990 Fusion Technology **17** 86

Söldner F X et al 1988 Phys. Rev. Lett. **61** 1105

Strachan J D et al 1987 Phys. Rev. Lett. **58** 1004

Takenaga H 1993 to be submitted to Nuclear Fusion

Uchino K et al 1992 Journal of Nuclear Materials **196-198** 210

Wagner F et al 1993 Plasma Phys. Control. Fusion **35** 1321

Ware A A 1970 Phys. Rev. Lett. **25** 15

Yamada H et al 1991 Controlled Fusion and Plasma Physics, Proc. 18th European Conf.

(Berlin) vol 15C pt II p137

------------------1992 Nuclear Fusion **32** 25

Figure Captions

Fig. 1 The peaking parameter of electron density(a) and temperature profiles (b), the central toroidal rotation velocity and the poloidal rotation velocity at $r = 2a/3$ (c) and the electron thermal diffusivity at half plasma radius (d) as a function of the position of the vacuum magnetic axis. The peaking parameter for electron density and toroidal/poloidal rotations in co-injection are also shown for comparison.

Fig. 2 The comparison of the electron temperature and density profiles for two different magnetic configurations together with the comparison of radial profiles of particle fluxes.

Table 1

Density Profile	Peaked Rax = 92.1 cm	Flattened Rax = 99.5 cm
D	0.4 m^2/s	----------
V_{in}	2 m/s	- 4 m/s
T_e'/T_e	18 m^{-1}	16 m^{-1}
E_r	Negative ($\|E_r\|$<5 kV/m)	Negative ($\|E_r\|$<5 kV/m)

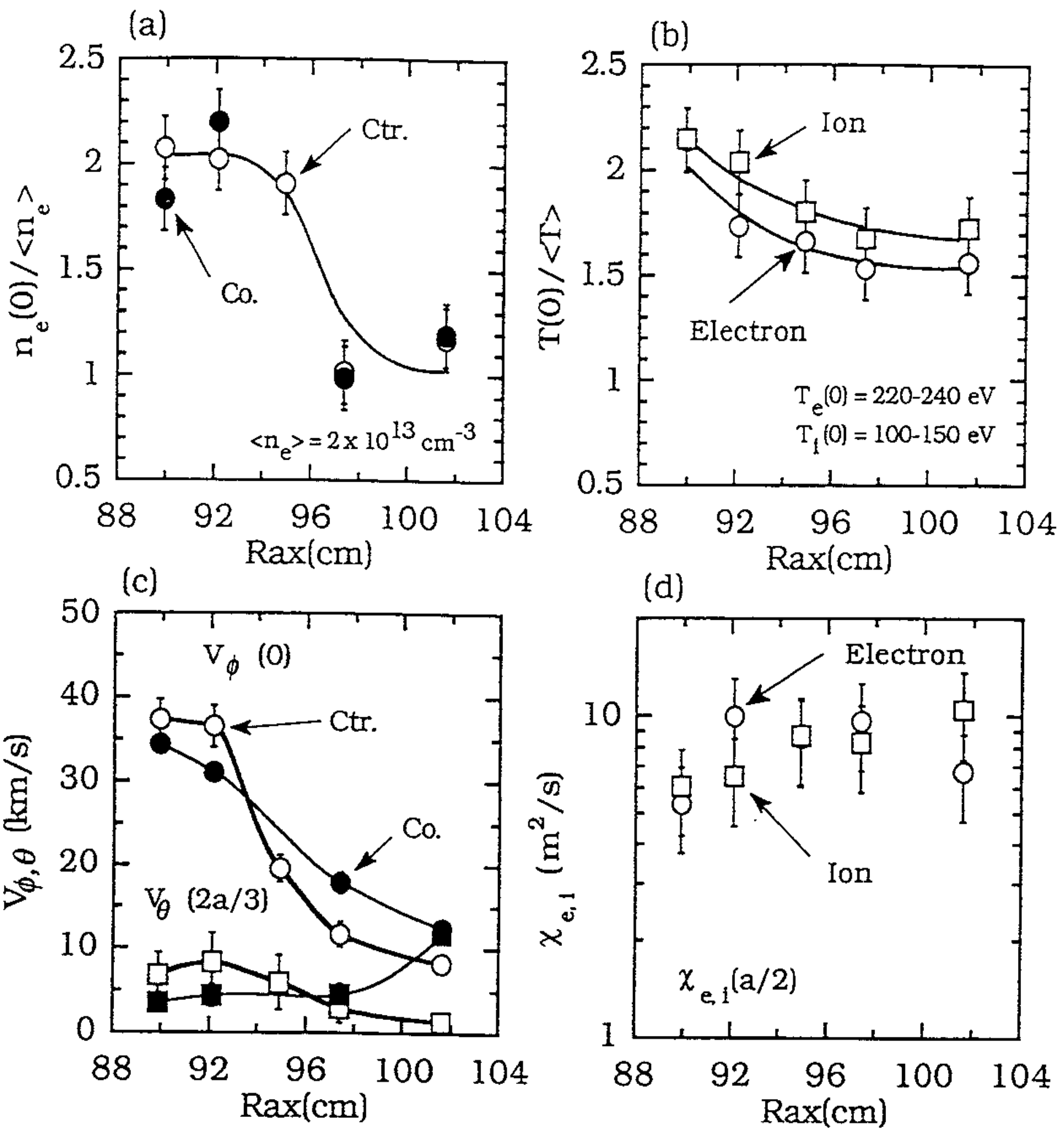

(a)
n_e(0)/<n_e>
Ctr.
Co.
<n_e> = 2 x 10^13 cm^-3
Rax(cm)
(b)
T(0)/<T>
Ion
Electron
T_e(0) = 220-240 eV
T_i(0) = 100-150 eV
Rax(cm)
(c)
V_φ,θ (km/s)
V_φ (0)
Ctr.
Co.
V_θ (2a/3)
Rax(cm)
(d)
χ_e,i (m^2/s)
Electron
Ion
χ_e,i(a/2)
Rax(cm)

Fig. 1

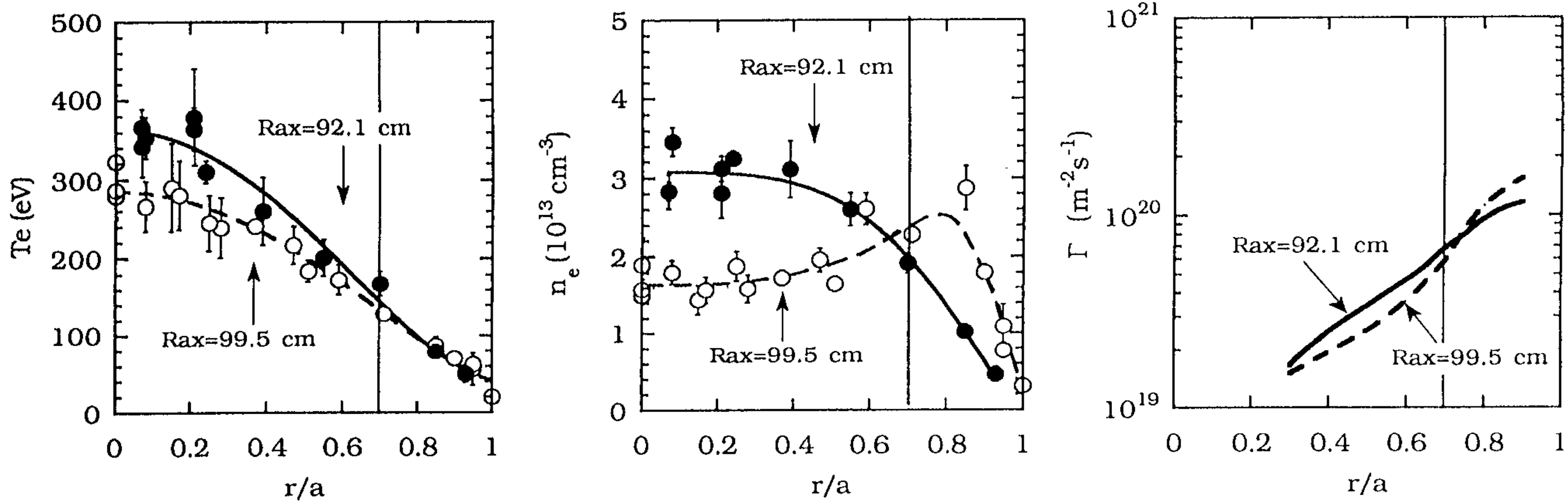

Te (eV)
500
400
300
200
100
0
Rax=92.1 cm
Rax=99.5 cm
0
0.2
0.4
0.6
0.8
1
r/a
n_e (10^{13} cm^{-3})
5
4
3
2
1
0
Rax=92.1 cm
Rax=99.5 cm
0
0.2
0.4
0.6
0.8
1
r/a
Γ ($m^{-2}s^{-1}$)
10^{21}
10^{20}
10^{19}
Rax=92.1 cm
Rax=99.5 cm
0
0.2
0.4
0.6
0.8
1
r/a

Fig. 2

Recent Issues of NIFS Series

NIFS-217 J. Guasp, K. Yamazaki and O. Motojima, *Particle Orbit Analysis for LHD Helical Axis Configurations* ; Apr. 1993

NIFS-218 T. Yabe, T. Ito and M. Okazaki, *Holography Machine HORN-1 for Computer-aided Retrieve of Virtual Three-dimensional Image* ; Apr. 1993

NIFS-219 K. Itoh, S.-I. Itoh, A. Fukuyama, M. Yagi and M. Azumi, *Self-sustained Turbulence and L-Mode Confinement in Toroidal Plasmas* ; Apr. 1993

NIFS-220 T. Watari, R. Kumazawa, T. Mutoh, T. Seki, K. Nishimura and F. Shimpo, *Applications of Non-resonant RF Forces to Improvement of Tokamak Reactor Performances Part I: Application of Ponderomotive Force* ; May 1993

NIFS-221 S.-I. Itoh, K. Itoh, and A. Fukuyama, *ELMy-H mode as Limit Cycle and Transient Responses of H-modes in Tokamaks* ; May 1993

NIFS-222 H. Hojo, M. Inutake, M. Ichimura, R. Katsumata and T. Watanabe, *Interchange Stability Criteria for Anisotropic Central-Cell Plasmas in the Tandem Mirror GAMMA 10 ;* May 1993

NIFS-223 K. Itoh, S.-I. Itoh, M. Yagi, A. Fukuyama and M. Azumi, *Theory of Pseudo-Classical Confinement and Transmutation to L-Mode;* May 1993

NIFS-224 M. Tanaka, *HIDENEK: An Implicit Particle Simulation of Kinetic-MHD Phenomena in Three-Dimensional Plasmas;* May 1993

NIFS-225 H. Hojo and T. Hatori, *Bounce Resonance Heating and Transport in a Magnetic Mirror;* May 1993

NIFS-226 S.-I. Iton, K. Itoh, A. Fukuyama, M. Yagi, *Theory of Anomalous Transport in H-Mode Plasmas;* May 1993

NIFS-227 T. Yamagishi, *Anomalous Cross Field Flux in CHS ;* May 1993

NIFS-228 Y. Ohkouchi, S. Sasaki, S. Takamura, T. Kato, *Effective Emission and Ionization Rate Coefficients of Atomic Carbons in Plasmas;* June 1993

NIFS-229 K. Itoh, M. Yagi, A. Fukuyama, S.-I. Itoh and M. Azumi, *Comment on 'A Mean Field Ohm's Law for Collisionless Plasmas;* June 1993

NIFS-230 H. Idei, K. Ida, H. Sanuki, H. Yamada, H. Iguchi, S. Kubo, R. Akiyama,

H. Arimoto, M. Fujiwara, M. Hosokawa, K. Matsuoka, S. Morita, K. Nishimura, K. Ohkubo, S. Okamura, S. Sakakibara, C. Takahashi, Y. Takita, K. Tsumori and I. Yamada, *Transition of Radial Electric Field by Electron Cyclotron Heating in Stellarator Plasmas;* June 1993

NIFS-231 H.J. Gardner and K. Ichiguchi, *Free-Boundary Equilibrium Studies for the Large Helical Device,* June 1993

NIFS-232 K. Itoh, S.-I. Itoh, A. Fukuyama, H. Sanuki and M. Yagi, *Confinement Improvement in H-Mode-Like Plasmas in Helical Systems,* June 1993

NIFS-233 R. Horiuchi and T. Sato, *Collisionless Driven Magnetic Reconnection,* June 1993

NIFS-234 K. Itoh, S.-I. Itoh, A. Fukuyama, M. Yagi and M. *Azumi, Prandtl Number of Toroidal Plasmas;* June 1993

NIFS-235 S. Kawata, S. Kato and S. Kiyokawa , *Screening Constants for Plasma;* June 1993

NIFS-236 A. Fujisawa and Y. Hamada, *Theoretical Study of Cylindrical Energy Analyzers for MeV Range Heavy Ion Beam Probes;* July 1993

NIFS-237 N. Ohyabu, A. Sagara, T. Ono, T. Kawamura and O. Motojima, *Carbon Sheet Pumping;* July 1993

NIFS-238 K. Watanabe, T. Sato and Y. Nakayama, *Q-profile Flattening due to Nonlinear Development of Resistive Kink Mode and Ensuing Fast Crash in Sawtooth Oscillations;* July 1993

NIFS-239 N. Ohyabu, T. Watanabe, Hantao Ji, H. Akao, T. Ono, T. Kawamura, K. Yamazaki, K. Akaishi, N. Inoue, A. Komori, Y. Kubota, N. Noda, A. Sagara, H. Suzuki, O. Motojima, M. Fujiwara, A. Iiyoshi, *LHD Helical Divertor;* July 1993

NIFS-240 Y. Miura, F. Okano, N. Suzuki, M. Mori, K. Hoshino, H. Maeda, T. Takizuka, JFT-2M Group, K. Itoh and S.-I. Itoh, *Ion Heat Pulse after Sawtooth Crash in the JFT-2M Tokamak;* Aug. 1993

NIFS-241 K. Ida, Y.Miura, T. Matsuda, K. Itoh and JFT-2M Group, *Observation of non Diffusive Term of Toroidal Momentum Transport in the JFT-2M Tokamak;* Aug. 1993

NIFS-242 O.J.W.F. Kardaun, S.-I. Itoh, K. Itoh and J.W.P.F. Kardaun, *Discriminant Analysis to Predict the Occurrence of ELMS in H-Mode Discharges;* Aug. 1993

NIFS-243 K. Itoh, S.-I. Itoh, A. Fukuyama,

Modelling of Transport Phenomena; Sep. 1993

NIFS-244 J. Todoroki,
Averaged Resistive MHD Equations; Sep. 1993

NIFS-245 M. Tanaka,
The Origin of Collisionless Dissipation in Magnetic Reconnection; Sep. 1993

NIFS-246 M. Yagi, K. Itoh, S.-I. Itoh, A. Fukuyama and M. Azumi,
Current Diffusive Ballooning Mode in Seecond Stability Region of Tokamaks; Sep. 1993

NIFS-247 T. Yamagishi,
Trapped Electron Instabilities due to Electron Temperature Gradient and Anomalous Transport; Oct. 1993

NIFS-248 Y. Kondoh,
Attractors of Dissipative Structure in Three Disspative Fluids; Oct. 1993

NIFS-249 S. Murakami, M. Okamoto, N. Nakajima, M. Ohnishi, H. Okada,
Monte Carlo Simulation Study of the ICRF Minority Heating in the Large Helical Device; Oct. 1993

NIFS-250 A. Iiyoshi, H. Momota, O. Motojima, M. Okamoto, S. Sudo, Y. Tomita, S. Yamaguchi, M. Ohnishi, M. Onozuka, C. Uenosono,
Innovative Energy Production in Fusion Reactors; Oct. 1993

NIFS-251 H. Momota, O. Motojima, M. Okamoto, S. Sudo, Y. Tomita, S. Yamaguchi, A. Iiyoshi, M. Onozuka, M. Ohnishi, C. Uenosono,
Characteristics of D-^3He Fueled FRC Reactor: ARTEMIS-L, Nov. 1993

NIFS-252 Y. Tomita, L.Y. Shu, H. Momota,
Direct Energy Conversion System for D-^3He Fusion, Nov. 1993

NIFS-253 S. Sudo, Y. Tomita, S. Yamaguchi, A. Iiyoshi, H. Momota, O. Motojima, M. Okamoto, M. Ohnishi, M. Onozuka, C. Uenosono,
Hydrogen Production in Fusion Reactors, Nov. 1993

NIFS-254 S. Yamaguchi, A. Iiyoshi, O. Motojima, M. Okamoto, S. Sudo, M. Ohnishi, M. Onozuka, C. Uenosono,
Direct Energy Conversion of Radiation Energy in Fusion Reactor, Nov. 1993

NIFS-255 S. Sudo, M. Kanno, H. Kaneko, S. Saka, T. Shirai, T. Baba,
Proposed High Speed Pellet Injection System "HIPEL" for Large Helical Device

Nov. 1993

NIFS-256 S. Yamada, H. Chikaraishi, S. Tanahashi, T. Mito, K. Takahata, N. Yanagi, M. Sakamoto, A. Nishimura, O. Motojima, J. Yamamoto, Y. Yonenaga, R. Watanabe,
Improvement of a High Current DC Power Supply System for Testing the Large Scaled Superconducting Cables and Magnets; Nov. 1993

NIFS-257 S. Sasaki, Y. Uesugi, S. Takamura, H. Sanuki, K. Kadota,
Temporal Behavior of the Electron Density Profile During Limiter Biasing in the HYBTOK-II Tokamak; Nov. 1993

NIFS-258 K. Yamazaki, H. Kaneko, S. Yamaguchi, K.Y. Watanabe, Y.Taniguchi, O.Motojima, LHD Group,
Design of Central Control System for Large Helical Device (LHD); Nov. 1993

NIFS-259 K. Yamazaki, H. Kaneko, S. Yamaguchi, K.Y. Watanabe, Y.Taniguchi, O.Motojima, LHD Group,
Design of Central Control System for Large Helical Device (LHD); Nov. 1993

NIFS-260 B.V.Kuteev,
Pellet Ablation in Large Helical Device; Nov. 1993

NIFS-261 K. Yamazaki,
Proposal of "MODULAR HELIOTRON': Advanced Modular Helical System Compatible with Closed Helical Divertor; Nov. 1993

NIFS-262 V.D.Pustovitov,
Some Theoretical Problems of Magnetic Diagnostics in Tokamaks and Stellarators; Dec. 1993

NIFS-263 A. Fujisawa, H. Iguchi, Y. Hamada
A Study of Non-Ideal Focus Properties of 30° Parallel Plate Energy Analyzers; Dec. 1993

NIFS-264 K. Masai,
Nonequilibria in Thermal Emission from Supernova Remnants; Dec. 1993

NIFS-265 K. Masai, K. Nomoto,
X-Ray Enhancement of SN 1987A Due to Interaction with its Ring-like Nebula; Dec. 1993

NIFS-266 J. Uramoto
A Research of Possibility for Negative Muon Production by a Low Energy Electron Beam Accompanying Ion Beam; Dec. 1993